Experimental Identification of Modal Momentum Coefficients and Modal Identity Parameters

Y. Soucy,* F. R. Vigneron,† and T. Steele‡
Canadian Space Agency, Ottawa, Ontario, Canada

The identification from laboratory test data of modal momentum coefficients, modal identity parameters, and conventional modal parameters (frequencies, damping factors, mode shapes, and modal normalization constants) is successfully demonstrated using recently developed theoretical procedures that are based on driven-base and portable exciter modal tests. The tests and demonstration employ a cantilever beam with unidirectional driven-base excitation. The use of experiment-derived modal parameters with modal identities to obtain a measurement-based assessment of relative modal momenta and completeness of the modal determination also is demonstrated. The results of three independent sets of data are compared with each other and with corresponding theoretical results for an undamped uniform cantilever beam.

Introduction

IN the driven-base modal test, the structure under test is attached to a rigid platform (base) that is driven by a powerful electrodynamic or hydraulic exciter system. The input measurement is made with accelerometers mounted to the base, and the measured outputs are accelerations at several points on the structure. The more familiar conventional modal test with portable exciters involves supporting the structure with respect to a nonmovable reference, measured inputs that are forces measured with load cells, and measured outputs that are accelerations.

In Ref. 1, it was demonstrated by numerical modeling and simulation that "moment of mode shape" type of modal parameters, as well as modal parameters identified in conventional modal tests (modal frequencies, damping factors, shapes, and normalization constants) can in theory be identified from a combination of data from driven-base modal tests and supplemental partial conventional (portable exciter) modal tests. Experimental identification of the additional types of modal parameters opens the way for assessment solely from test data of the relative importance of modes and for their use in validation of analytical models. Also, "moment of mode shape" parameters appear naturally in analytical models of space vehicle dynamics; therefore it is of interest to have a means of direct identification of them that does not rely on assumptions of analytical modeling.

The following specific principles are described in Ref. 1. The driven-base test configuration with translational excitation in the x direction provides data that enable the estimation of the following modal parameters for each mode: natural frequency, damping ratio, mode shape, the product $Q_k \mathcal{P}_{xk}$, where Q_k and $\mathcal{P}_{xk}$ are, respectively, the modal normalization constant and linear modal momentum coefficient (i.e., the first moment of the mode shape) in the x direction of a kth mode. A modal test with a force input and a small number of output accelerometers (referred to herein as a "partial" modal test) suffices to estimate the Q_k, provided that the excitation point is not a node and the output signal contains a sufficiently high content of response of each mode. With the products $Q_k \mathcal{P}_{xk}$ estimated from data of a driven-base test and the Q_k estimated from a partial modal test, it is possible to construct estimates of $\mathcal{P}_{xk}$ by dividing $Q_k \mathcal{P}_{xk}$ by Q_k. These measurement-derived $\mathcal{P}_{xk}$ and Q_k can be further used to calculate estimates of modal quantities that are associated with modal identities for damped natural modes; such "modal identity parameters" can be used in turn to assess the relative significance of individual modes and the overall completeness of the experimental modal determination. These principles have been demonstrated by computer simulation of a structure in Ref. 1. Similar principles are also partially explored in theory and by simulation in Refs. 2 and 3. The estimation of modal frequencies and shapes from driven-base data has been demonstrated to some extent in Refs. 4 and 5, but estimation of the momentum coefficient and modal identity parameters has not been demonstrated yet with laboratory data from real structures.

The purpose of this paper is to report on the experimental demonstration with a cantilever beam structure of the principles of the preceding paragraphs and, in particular, those relating to modal momentum coefficients, parameters of the modal identities, and modal damping factors. In the following, the main equations for parameter estimation and modal identities are summarized first. Then, corresponding driven-base and partial modal survey tests and results for an instrumented cantilever steel beam are described. Measurement-derived estimates of the various parameters are obtained and their use with modal identities is demonstrated. Three independent data sets for the beam are obtained, and the associated estimated parameters are compared. The corresponding theoretical results for an idealized undamped uniform cantilever beam also are examined as a point of reference.

Estimation Concepts and Procedures

The theory and assumptions underlying the modeling and corresponding parameter estimation for driven-base and modal survey tests are presented in detail in Ref. 1. The following summary describes the concepts and notation to the extent necessary to present and discuss the experimental work of later sections.

A structure undergoing driven-base modal test is illustrated schematically in Fig. 1. The base is assumed driven in a single direction Ox with no rotation. The reference axes (Ox, Oy, Oz) are fixed to an arbitrary convenient location of the driven

Received July 20, 1987; revision received May 10, 1988.

*Research Engineer. Member AIAA.
†Research Scientist. Member AIAA.
‡Senior Technologist.

base. The deformation of each mass point of the structure is defined relative to the driven base by components (u^i, v^i, w^i) in the (Ox, Oy, Oz) reference frame. The measurable quantities upon which parameter estimation is based are 1) the input acceleration $a_0(t)$ equal to $\ddot{\Xi}(t)$ and 2) the inertial accelerations at each mass point denoted by $\{a_x^i(t), a_y^i(t), a_z^i(t)\}$, where t denotes time, an independent variable. The analytical model of this test configuration can be described in the frequency domain by

$$\frac{1}{\omega^2}\begin{bmatrix} \bar{A}_x(\omega)/\bar{a}_0(\omega) - \Sigma \\ \bar{A}_y(\omega)/\bar{a}_0(\omega) \\ \bar{A}_z(\omega)/\bar{a}_0(\omega) \end{bmatrix} = \sum_{k=1}^{n}\left\{\frac{Q_k \mathcal{P}_{xk}\Phi_k}{i\omega - \lambda_k} + \frac{Q_k^* \mathcal{P}_{xk}^*\Phi_k^*}{i\omega - \lambda_k^*}\right\} \quad (1)$$

In Eq. (1), $A_x^T = [a_x^1, a_x^2, \ldots, a_x^N]$ and $\Sigma^T = [1,1,\ldots,1]$; A_x, Σ, etc., are all of order $N \times 1$, where N is the number of mass points of the assumed model for the structure, and ω denotes the frequency, an independent variable. Modal parameters of the kth mode are λ_k, Φ_k, Q_k, and $\mathcal{P}_{xk}$; n is equal to $3N$. A modal eigenvalue λ_k is related to its modal frequency ω_k and damping ratio ζ_k by $\lambda_k = -\zeta_k\omega_k + i\omega_k(1-\zeta_k^2)^{1/2}$. The Q_k are modal normalization constants. The linear modal momentum coefficient P_{xk} is defined by

$$\mathcal{P}_{xk} = \sum_{i=1}^{N} m^i \theta_k^i \quad (2)$$

where m^i is the mass of the ith point and θ_k^i the component in the Ox direction of the kth mode shape associated with m^i; $\mathcal{P}_{xk}$ also might be described as a first moment of the kth mode shape about the Ox axis. The parameters Q_k, $\mathcal{P}_{xk}$, θ_k^i, Φ_k, and λ_k are complex valued, and the * denotes the complex conjugate. Equation (1) relates the modal parameters (right-hand side, λ_k, Φ_k, Q_k, and $\mathcal{P}_{xk}$, $k = 1$ to n) to the quantities that are directly measurable (left-hand side, A and a_0) and is the basic model needed for parameter estimation by curve-fitting methods for driven-base tests with single-degree-of-freedom excitation in the Ox direction. Equation (1) corresponds to a passive structure with general linear viscous (not proportional) damping.

Estimates of the functions $A_x(\omega)/\bar{a}_0(\omega)$, $\bar{A}_y(\omega)/\bar{a}_0(\omega)$, and $\bar{A}_z(\omega)/\bar{a}_0(\omega)$ may be obtained from the accelerometer data of a test using standard data acquisition and spectral analysis equipment. From these quantities, a measurement-based estimate of the functions appearing on the left-hand side of Eq. (1) may be constructed. Modal parameter estimation then entails determination of the values of the modal parameter set λ_k, Φ_k, $(Q_k\mathcal{P}_{xk})$ that result in an acceptable curve fit of Eq. (1) to the measurement-based estimate of the functions.

For the driven-base test, the kth mode shape is normalized so that ϕ_k^d is unity, where ϕ_k^d refers to the dth component of Φ_k. There is not enough information to deduce separate estimates of Q_k and $\mathcal{P}_{xk}$ solely from the data of the driven-base tests.

When the estimation procedure for the modal survey test is modeled using a nonproportionally damped model in an analytical development that parallels that of the preceding paragraphs, the modal parameters that are estimated are the set λ_k, Φ_k, Q_k. The Q_k are conceptually similar to the modal masses of the conventional modal survey test that is based on a proportionally damped structural model.

A driven-base test with excitation in the Ox direction provides an estimate of the products $Q_k\mathcal{P}_{xk}$, and a partial modal survey provides an estimate of Q_k. Then, an estimate of the linear modal momenta $\mathcal{P}_{xk}$ can be obtained by dividing the two estimates.

The modal identity involving the Ox-associated linear momentum coefficients may be written in the form

$$\sum_{k=1}^{n} \mathfrak{M}_{xx}^k \leq m \quad (3)$$

where $\mathfrak{M}_{xx}^k$ are "modal identity parameters" defined by

$$\mathfrak{M}_{xx}^k = \lambda_k Q_k \mathcal{P}_{xx}^2 + \lambda_k^* Q_k^* P_{xk}^{*2} \quad (4)$$

Estimates of λ_k, Q_k, and $\mathcal{P}_{xk}$ can be derived from tests as outlined in the foregoing, and from them measurement-based estimates for $\mathfrak{M}_{xx}^k$ can be calculated using Eq. (4); $\mathfrak{M}_{xx}^k$ is a measure of the net linear momentum associated with the kth vibratory mode and also is invariant to the choice of modal normalization constant of Φ_k. Comparison of the individual $\mathfrak{M}_{xx}^k$, $k = 1,2$, etc., indicates the relative linear momentum in the Ox direction of each mode. The mass m of the structure can be estimated by weighing it. Equation (3) states that the sum of the experimentally derived $\mathfrak{M}_{xx}^k$ should equal m; the extent to which it does indicates the accuracy of the experimental modal determination process.

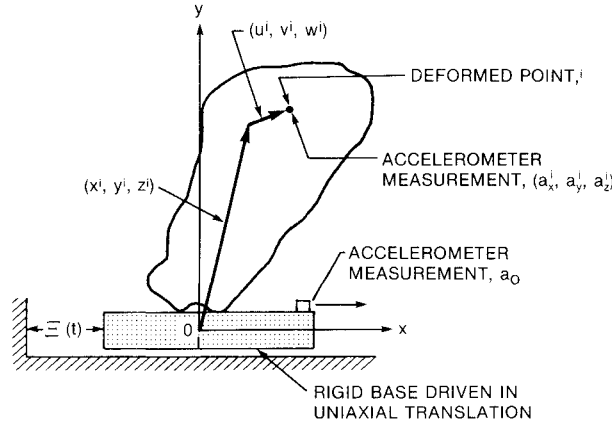

Fig. 1 Schematic of driven-base test configuration.

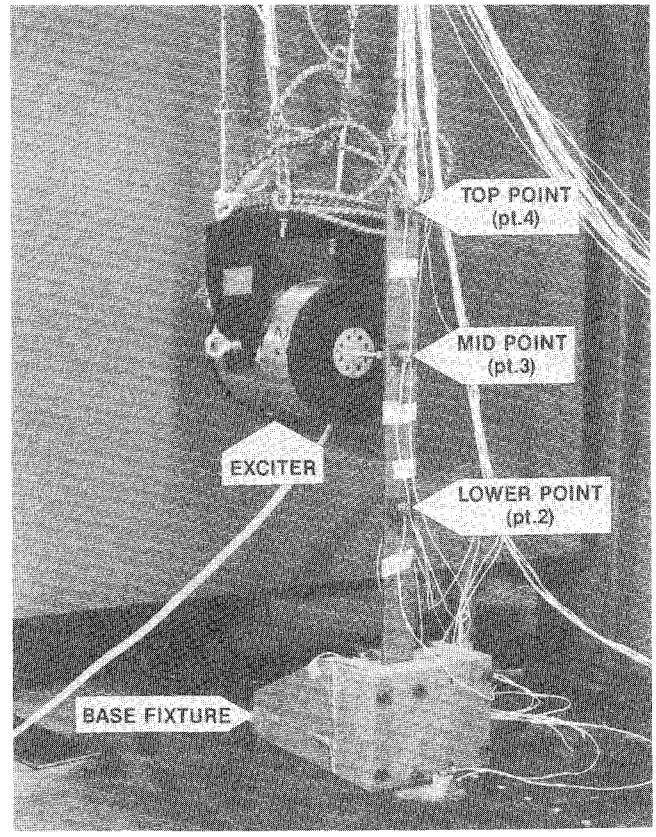

Fig. 2 Experimental steel beam in test configuration.

Experimental Results

Test Structure, Instrumentation, and Facilities

A cantilever beam was chosen as the structure upon which to attempt the laboratory demonstration of the foregoing concepts. This type of structure was chosen so as to avoid undue complexity in geometry and amount of instrumentation, and because exact theoretical results of an ideal uniform undamped beam are well known and readily available as a comparison guide.

Modes in one lateral direction only (by definition the Ox direction) were excited and measured. Three reference points on the beam were selected, namely at the tip and at two-thirds and one-third of the length (designed as points 4, 3, and 2, respectively). This allowed the driven-base test and three independent single-input partial modal survey tests to be conducted. This combination of tests enables four independent experimental estimates of the modal frequencies and damping factors, and three independent experimental estimates of the $\mathfrak{M}_{xx}^{k}$ and their sums, to be used for comparison purposes.

A photograph of the beam and elements of various test configurations is given in Fig. 2. The beam was mounted to its base (an isolation mass, in the photograph) by means of a base fixture. The beam was 61 cm long, 5.1 cm wide, and 0.635 cm thick and was made of steel. Three accelerometers and associated cabling were mounted permanently to the beam for all tests. Also shown in the photograph are the portable exciter and load cell that were used in the independent partial modal survey tests.

The type of accelerometers was selected to minimize their mass relative to the mass of the beam while being sensitive enough to produce a good signal to noise ratio response. The base fixture was designed to be as rigid as practicable to attain a fixed boundary condition. Additional accelerometers also were mounted to the fixture to monitor any unexpected deformations or motions of it.

The relevant masses of the test setup were a 1530 g beam, three accelerometers totaling 50 g, and a 20 g force transducer for a total of 1600 g.

The data were acquired and preprocessed with a commercially available Fourier system configured with 16 digital-to-analog channels, so the response signals of all three measurement points could be taken simultaneously. Efforts were made to obtain the most accurate measurements possible. Each measurement channel (sensor through analog-to-digital converter of the analyzer) was calibrated prior to the tests.

Estimation of ω_k, ζ_k, and $Q_k\mathcal{P}_{xk}$ Using Driven-Base Testing

The driven-base tests were done with the beam mounted to the slip table of a 27 kN exciter. The base was excited with a random signal, and its motion was measured with an accelerometer.

Figure 3 shows an example of a baseband frequency response function containing peaks of all four measured modes. The modes are seen to be well separated. Due to low damping of the beam and in order to increase the accuracy of the estimation, the data from which modal parameters were estimated consisted of frequency response functions zoomed around each peak sequentially (i.e., the 512 frequency lines were located in a narrow bandwidth around the natural frequency of interest).

The parameter estimation was done using a complex exponentials algorithm of a commercially available software[6] to curve fit the data. An estimate of the λ_k was obtained first by curve fitting simultaneously all three frequency response functions of a run. Then, estimates of the elements of the mode shape vector were obtained sequentially from these response functions. The shape coefficients also were estimated with a circle fit technique for most modes and confirmed the ones from the complex exponentials routine.

The frequency values obtained from driven-base testing are presented in the second column of Table 1. Damping estimates

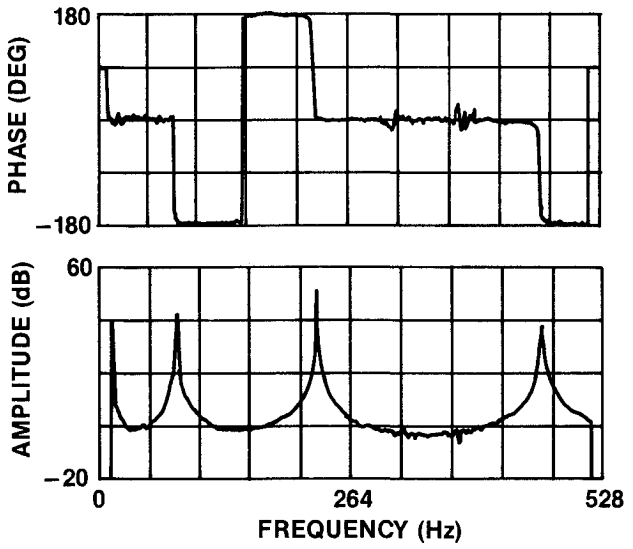

Fig. 3 Frequency response function of point 4 from driven-base test.

Table 1 Modal frequencies, Hz

Mode	Driven base	Modal test Pt 2	Modal test Pt 3	Modal test Pt 4	Theoretical undamped
1	13.33	13.37	13.76	13.18	13.77
2	82.70	83.49	83.45	83.16	86.28
3	229.8	232.3	232.3	232.0	241.6
4	465.5	465.0	464.8	462.3	473.4

Table 2 Damping ratios, %

Mode	Driven base	Modal test Pt 2	Modal test Pt 3	Modal test Pt 4
1	0.079	0.086	0.260	0.032
2	0.131	0.064	0.095	0.174
3	0.152	0.080	0.085	0.093
4	0.167	0.174	0.156	0.161

Table 3 Product $Q_k\mathcal{P}_{xk}$,s

Mode	Driven base Amplitude	Driven base Phase, deg	Theoretical undamped Amplitude	Theoretical undamped Phase, deg
	Derived from point 2			
1	0.00178	−90.0	0.00155	−90
2	0.000535	−90.2	0.000481	−90
3	0.000122	−89.9	0.000119	−90
4	0.00000554	−84.3	0.00000885	−90
	Derived from point 3			
1	0.00531	−90.2	0.00499	−90
2	0.000345	−90.2	0.000329	−90
3	0.000111	90.9	0.000109	90
4	0.0000107	−93.0	0.0000122	−90
	Derived from point 4			
1	0.00907	−89.7	0.00883	−90
2	0.000695	90.3	0.000733	90
3	0.000131	−89.2	0.000144	−90
4	0.0000405	91.0	0.0000490	90

are given in the second column of Table 2. These values correspond to percentage of critical damping assuming a linear viscous model. Table 3 presents estimates of the products of $Q_k\mathcal{P}_{xk}$ derived from the three point locations. The results contained in the tables will be discussed and compared with the other data in the tables in a subsequent section.

Estimation of ω_k, ζ_k, and Q_k Using Modal Testing

The base fixture and the beam were mounted to an isolation mass of more than 900 kg for the partial modal survey tests. A random excitation was input sequentially at the three driving points by a portable exciter through a plastic stinger rod and a force transducer. The data were taken by zooming with the same bandwidth as for the driven-base tests.

The estimated frequencies are presented in columns 3-5 of Table 1. Damping values are given in the same columns of Table 2. The estimated normalization constants Q_k are shown in columns 2 and 3 of Table 4.

Experiment-Based Estimation of $\mathcal{P}_{xk}$ and $\mathfrak{M}^k_{xx}$

The experimental linear modal momentum values $\mathcal{P}_{xk}$ are shown in Table 5. These values were obtained by dividing the estimated $Q_k\mathcal{P}_{xk}$ by the estimated Q_k.

Table 6 contains the experiment-based $\mathfrak{M}^k_{xx}$ and their sums. These estimated values are obtained using Eq. (4) and estimated parameters of Tables 1, 2, 4, and 5.

Calculation of Theoretical Modal Parameters of the Beam

The theoretical values of the various modal parameters (λ_k, Q_k, $\mathcal{P}_{xk}$, $Q_k\mathcal{P}_{xk}$, and $\mathfrak{M}^k_{xx}$) were calculated based on the well-known continuum theory of flexural vibration for a uniform undamped cantilever beam (described in Ref. 7, for example).

In this case, $\lambda_k = i\omega_k$ and $\theta_k(y)$ are real valued. Reference 7 tabulates the values of frequencies and the corresponding mode shapes as continuous functions of y. The linear modal momenta P_{xk} are given by the counterpart of Eq. (2) for the continuous model

$$\mathcal{P}_{xk} = \int_0^l \rho\theta_k(y)\,dy \tag{5}$$

where l and ρ are, respectively, the length and mass per unit length of the beam. Since θ_k are real, the theoretical $\mathcal{P}_{xk}$ are real, with phase of either 0 or 180 deg.

The modal normalization constants are given by

$$Q_k = \left[2i\omega_k\rho\int_0^l \theta_k^2(y)\,dy\right]^{-1} \tag{6}$$

where ω_k are the natural frequencies. The phases of the Q_k are always equal to -90 deg for the undamped model.

For the undamped continuous model, $\mathfrak{M}^k_{xx}$ can be shown to be expressed as

$$\mathfrak{M}^k_{xx} = \left[\int_0^l \rho\theta_k(y)\,dy\right]^2 \Big/ \int_0^l \rho\theta_k^2(y)\,dy \tag{7}$$

Since θ_k are real, $\mathfrak{M}^k_{xx}$ are real. Also, $\mathfrak{M}^k_{xx}$ are seen to be invariant to the choice of scale factor of θ_k.

The theoretical values of the various quantities are given in Tables 1, 3, 4, 5, and 7.

Discussion of Results

Regarding the frequency values presented in Table 1, the most significant observation is the consistency of the discrepancy between the experimental and theoretical values. For the first three modes, the experimental frequencies (driven-base and modal survey) are 3-5% lower than the theoretical values; the difference is less for the last mode. The differences are due to identifiable inadequacies in the model. One of the causes is a small unmodeled flexibility of the base, which was also observed with accelerometers. Other possible causes are a small unmodeled flexibility of the fixture, error in the value of Young's modulus E (E of 193 GPa was used), and unmodeled shear force effects.

For the modal survey, the three estimates of frequency are in very good agreement, except for mode 1 for which there is a difference of more than 4% between the extreme values. These estimates are close to the values from driven-base tests.

Table 4 Modal normalization constant Q_k, s/kg

Mode	Modal survey		Theoretical undamped	
	Amplitude	Phase, deg	Amplitude	Phase, deg
	Derived from point 2			
1	0.000430	−91.8	0.000445	−90
2	0.000784	−91.6	0.000873	−90
3	0.000359	−91.8	0.000435	−90
4	0.00000403	−103.9	0.00000924	−90
	Derived from point 3			
1	0.00432	−90.3	0.00462	−90
2	0.000379	−91.1	0.000408	−90
3	0.000307	−92.1	0.000363	−90
4	0.0000105	−95.7	0.0000175	−90
	Derived from point 4			
1	0.0135	−93.5	0.0144	−90
2	0.00164	−91.0	0.00202	−90
3	0.000459	−91.2	0.000642	−90
4	0.000186	−91.8	0.000283	−90

Table 5 Linear momentum coefficients $\mathcal{P}_{xk}$, kg

Mode	Experiment derived		Theoretical undamped	
	Amplitude	Phase, deg	Amplitude	Phase, deg
	Derived from point 2			
1	4.14	1.8	3.48	0
2	0.682	1.4	0.551	0
3	0.340	1.9	0.273	0
4	1.37	19.6	0.958	0
	Derived from point 3			
1	1.23	0.1	1.08	0
2	0.910	0.9	0.806	0
3	0.362	183.0	0.300	180
4	1.02	2.7	0.697	0
	Derived from point 4			
1	0.672	3.8	0.613	0
2	0.424	181.3	0.363	180
3	0.285	2.0	0.225	0
4	0.218	182.8	0.173	180

Table 6 Experiment derived $\mathfrak{M}^k_{xx}$, kg

Mode	Experiment derived		
	Point 2	Point 3	Point 4
1	1.229	1.081	1.042
2	0.380	0.340	0.332
3	0.120	0.125	0.124
4	0.040	0.063	0.064
Σ	1.769	1.609	1.562

Table 7 Comparison of measured and theoretical $\mathfrak{M}^k_{xx}$, kg

Mode	Experiment derived[a]	Theoretical undamped
1	1.062	0.981
2	0.336	0.301
3	0.124	0.104
4	0.063	0.053
5	Not measured	0.032
6	Not measured	0.021
7 − ∞	Not measured	0.108
Σ	1.585[b]	1.600[b]

[a]Average of points 3 and 4. [b]Mass of structure (beam plus instrumentation) equals 1.6 kg.

There are large discrepancies between the three different damping estimates of the modal survey shown in Table 2, especially for the first two modes for which the maximum values are about three times the lowest ones. Since the damping is quite small, one source of the variation in estimates could be the change in exciter setup associated with the different driving points. A further confirmed source was nonlinearity effects.[8] The damping estimates from the modal survey are different in many cases to the ones from driven-base tests (Table 2). In part, this could be due to the fact that the portable exciter and attachment of the modal survey tests are deleted completely during driven-base tests. Supplementary tests[8] also showed that damping estimates vary significantly depending on how the accelerometer cables are attached (hung freely, partly or fully attached to the structure). The cables were partly taped to the beam for the tests reported in this paper. They had to be disconnected and removed between the modal and driven-base tests, and hence part of the difference in damping is likely due to a lack of consistency in the attachment of the cables.

Table 3 contains the products $Q_k \mathcal{P}_{xk}$. The values of $Q_k \mathcal{P}_{xk}$ depend on the choice of normalization of the Φ_k. The choice of normalization is different for points 2–4, and therefore the respective $Q_k \mathcal{P}_{xk}$ shown in Table 3 cannot be cross compared. The estimated and theoretical values clearly correspond to each other, although there are numerical differences. The differences are consistent with the fact that there are discrepancies in frequencies (Table 1), which were attributed to unmodeled flexibility at the base. A further shortcoming in the modeling that could be of relevance in these tables is that the test results yield damped natural modes, whereas the theoretical ones are corresponding undamped natural modes.

The normalization constants Q_k are presented in Table 4. The experimental and theoretical values correspond, although there are discrepancies. The experimental values are always smaller than the theoretical ones. The shortcomings in the model noted earlier are the most likely sources of the differences.

Table 5 contains the linear momentum coefficients $\mathcal{P}_{xk}$. The experimental and theoretical values clearly correspond to each other. The estimates of the $\mathcal{P}_{xk}$ are obtained by dividing the estimates of $Q_k \mathcal{P}_{xk}$ (Table 3) by the corresponding estimates of Q_k (Table 4). Because of this, the discrepancies in $\mathcal{P}_{xk}$ are attributable to discrepancies in the other two parameters.

The most interesting comparisons are the $\mathfrak{M}_{xx}^k$ given in Tables 6 and 7. As was mentioned in the theoretical description, the value of $\mathfrak{M}_{xx}^k$ is independent of the scaling factor of a particular mode and thus of the choice of driving point of the modal survey test. This is of utmost importance since it permits the use of data of several driving points to cross-check the estimation of this parameter. In Table 6, it is observed that the estimates from driving points 3 and 4 are in very good agreement for all four modes with a difference less than 4%. The estimates from driving point 2 are similar to the other two estimates. The data for mode 4 at point 2 were noted to be associated with a poor curve fit, which would discount data from this point slightly. Good estimates of $\mathfrak{M}_{xx}^k$, entered in Table 7, are the average values of the estimates from points 3 and 4.

In Table 7, the experiment-derived values are presented beside the values for the uniform undamped cantilever beam. A definite correspondence is observed. The experiment-derived values are slightly higher than the corresponding theoretical values. Further, the sum of only four experiment-derived $\mathfrak{M}_{xx}^k$ essentially equals the mass of the structure. These discrepancies can be attributed to the aforementioned shortcomings in the theoretical model that were noted in data of other tables, namely: 1) the beam is not perfectly cantilevered at the base and 2) the driven-base did not move in pure translation, i.e., in addition a small rotation occurred. Consequently, the "mass of the structure" with which the summation of $\mathfrak{M}_{xx}^k$ should be compared also would include an undeterminable amount of the deforming base and fixture, in addition to the 1.6 kg of the beam and instrumentation.

Reference 9 also presents test data and analysis of the same beam and test configuration as reported herein. The work was based on different data taken from point 4 only and with less refined curve fitting, theoretical values, and load cell location. The data and analysis herein are more precise and supercede that of Ref. 9.

Conclusions

All aspects of the methods of Ref. 1 have been successfully demonstrated experimentally for unidirectional translational driven-base excitation in test of a cantilever beam.

Theoretical values are calculated from the theory of an undamped flexural cantilever beam and are used as a guideline. The experimental and calculated parameters are similar, although there are some differences. The differences are believed to be due mainly to unmodeled rotations and or deformations of the base, some deformations of the fixture, unmodeled shear force effects, damping effects, and error in Young's modulus.

The test results demonstrate very conclusively that independent estimates of the $\mathfrak{M}_{xx}^k$ can be obtained from different driving points and can be used to assess the quality of the estimation.

The results suggest that unmodeled movements of the base (rotations or deformations) produce an overestimation of the $\mathfrak{M}_{xx}^k$. In theory, the $\Sigma_{k=1}^n \mathfrak{M}_{xx}^k$ for all the modes should equal the mass of the structure under test. In practice, the mass of the structure may effectively and inadvertently include an undetermined fraction of the mass of the base and fixture.

On balance, these test results indicate that the driven-base test and associated techniques described in Ref. 1 show a great deal of promise. Further developments with certain aspects of the procedures are needed. Also, further testing of different more complex structures is warranted.

References

[1]Vigneron, F. R. and Soucy, Y., "Driven-Base Tests for Modal Parameter Estimation," *AIAA Journal,* Vol. 25, Jan. 1987, pp. 152–160.

[2]Matzen, V. C. and Murphy, C. E., "On Obtaining Mass Participation Factors Using 'Equivalent Structures'," *International Journal of Analytical and Experimental Modal Analysis,* Vol. 1, Jan. 1986, pp. 17–23.

[3]Link, M., "Structural System Identification Using Single and Multi-Axial Vibration Test Data," *Proceedings of Conference on Spacecraft Structures,* European Space Agency, Paris, SP-238, 1986, pp. 179–184.

[4]Béliveau, J.-G., Vigneron, F. R., Soucy, Y., and Draisey, S., "Modal Parameter Estimation from Base Excitation," *Journal of Sound and Vibration,* Vol. 107, No. 3, June 1986, pp. 435–449.

[5]Draisey, S., Vigneron, F. R., Soucy, Y., and Béliveau, J.-G., "Modal Parameter Estimation from Driven-Base Tests," *Second International Symposium on Aeroelasticity and Structural Dynamics,* DGLR, Bonn, FRG, April 1985.

[6]Leuridan, J. and Vold, H., "A Time-Domain Linear Modal Estimation Technique for Multiple Input Modal Analysis," *Modal Testing and Modal Refinement, American Society of Mechanical Engineers,* New York, AMD-Vol. 59, 1983, pp. 51–62.

[7]Bishop, R. E. D. and Johnson, D. C., *The Mechanics of Vibration,* Cambridge Univ. Press, London, 1979, Chap. 7.

[8]Soucy, Y. and Deering, D. W., "Effects of Data Acquisition Conditions on Modal Testing of a Simple Structure," *Proceedings of Sixth Modal Analysis Conference,* SEM, Bethel, CT, Feb. 1988, pp. 8–13.

[9]Soucy, Y., Vigneron, F. R., and Steele, T., "Experimental Results on Driven-Base Modal Parameter Estimation," *Proceedings of the Fifth Modal Analysis Conference,* SEM, Bethel, CT, April 1987, pp. 1151–1157.